To be presented at the International Meeting on Light-Water Reactor Severe Accident Evaluation, Cambridge, Mass., August 28-September 1, 1983

FISSION PRODUCT RELEASE FROM FUEL UNDER LWR ACCIDENT CONDITIONS

M. F. Osborne, R. A. Lorenz, K. S. Norwood,
J. L. Collins, and R. P. Wichner
Chemical Technology Division
Oak Ridge National Laboratory
Oak Ridge, Tennessee 37830

INTRODUCTION

Experimental studies of fission product release from commercial light-water reactor (LWR) fuel under the conditions of a severe accident are conducted under the sponsorship of the U.S. Nuclear Regulatory Commission (NRC). The test program was designed to provide the experimental data required for consequence evaluation in the analysis of reactor accidents. The specific objectives are (a) to determine fission product and aerosol release from fully-irradiated fuel under accident conditions, (b) to identify the chemical forms of the released material, and (c) to correlate the results with experiment and specimen conditions and with the data from related experiments (1-4). The test conditions are not intended to model specific accident sequences; the tests are conducted, rather, over a range of fuel operating histories, test times, temperatures, and steam flow rates, so that the data obtained are applicable to a spectrum of accident sequences in both boiling and pressurized water reactors. This paper considers the results of three experiments in the temperature interval 1400 to 2000°C, in which maximum fission product releases of >50% of the krypton, iodine, and cesium were observed. Additional tests at a variety of conditions will be conducted.

APPARATUS AND PROCEDURE

The experimental apparatus was constructed utilizing design features from several previous fuel testing programs (1,3,5). The induction furnace for heating the fuel specimens to 2000°C in flowing steam required a new design in which a tungsten or graphite susceptor is protected by a blanket of inert gas. Fission product collection and analysis techniques similar to those used by Lorenz et al. (1,2) were expanded to provide more detailed results. The principal analytical techniques are summarized in Table 1; gamma spectrometry is the most versatile and most widely-used of these methods. Other techniques have been, and will continue to be, investigated. The configuration of the test apparatus is illustrated in Fig. 1. On-line release data are obtained with NaI(Tl) detectors monitoring the thermal gradient tube, the filter package, and the cold charcoal traps. Following the test, quantitative data are obtained via gamma-ray spectrometry of all apparatus components. Additional data are obtained through mass spectrometry and activation analysis of samples from selected locations. Metallographic examination is used for evaluation of test effects on the UO_2 fuel and Zircaloy cladding.

RESULTS AND DISCUSSION

Three tests of PWR fuel have been conducted and evaluated, and the results have been reported in detail (6-8). Fuel specimen and test operating data for these three tests are presented in Table 2. The temperature and flow histories for a representative test (HI-2) are shown in Fig. 2. The peak in the flow rate out of the system (largely noncondensable hydrogen) at 18 min illustrates the rapid oxidation of the Zircaloy by steam during this period. In test HI-2, both the volume of hydrogen formed and subsequent metallographic examination indicated essentially complete oxidation of the cladding to ZrO_2. The release histories of cesium and krypton in this same test, as functions of time and temperature, are presented in Fig. 3. In this test the 160-g specimen was heated at about 1°/s to the test temperature of 1700°C, which was maintained for 20 min. (The raw data shown in Figs. 2 and 3 require small corrections to both the thermocouple and optical pyrometer values to obtain the true temperature.) The release curves for ^{85}Kr and ^{137}Cs (Fig. 3) show that these nuclides continued to be released from the furnace during cooldown. The release data for all three tests are summarized in Table 3. The iodine data were obtained by activation analysis of the long-lived ^{129}I in leach solutions. Because of the high radiation levels of ^{137}Cs (and also ^{134}Cs), other nuclides (such as ^{125}Sb, ^{110m}Ag, and ^{154}Eu) could not be measured until after most of the cesium had been chemically removed. As shown in Table 3, most of the material released from the furnace was collected either on the platinum-lined thermal gradient tube or on the fiberglass filters.

The relative distributions of cesium and iodine in the test HI-2 apparatus are illustrated in Fig. 4. These curves, which are typical of all three tests, show the higher mass of cesium at most locations, reflecting the higher inventory of cesium. The high concentration of cesium at the furnace outlet shifted with test temperatures, indicating condensation (or possibly reaction with the ZrO_2) at ~1200°C.

The thermal gradient tube is a quartz tube of 0.36-cm internal diameter and 36 cm long, lined with platinum foil to provide an inert deposition surface. Heating coils, monitored and controlled by thermocouples, impress an approximately linear temperature drop from 900°C at the gas inlet to 150°C at the gas outlet. Radionuclides deposit on the platinum and are detected by gamma spectrometry or by neutron activation of the

leach solutions. Figure 5 shows profiles for radionuclides measured in test HI-2.

Antimony was resistant to both basic and acidic leaches; thus, it must have combined chemically with the platinum. The amount of deposited antimony decreased exponentially with distance along the thermal gradient tube -- by a factor of 1000 in test HI-2. The gas phase concentration of antimony also declined, by a factor of 170 in this test. Such behavior may be explained as elemental antimony escaping from the fuel and reacting rapidly and irreversibly with the platinum surface of the thermal gradient tube, such that gas phase diffusion of antimony molecules limits the deposition rate. Apparently, temperature had little effect on the ratio of gas-phase to deposited antimony, which indicates an almost temperature independent process such as gas phase diffusion. If antimony was released at a constant rate during the test, it entered the thermal gradient tube at a partial pressure of 10^{-7} bar. At 850°C, the vapor pressure of antimony is about 4×10^{-3} bar (9), so the activity of deposited antimony must have been reduced by solution or reaction. We suggest this mechanism because antimony is known to form a solid solution in platinum below 10 atom % (10). As shown in Table 3, no measurable antimony was found outside the furnace in test HI-3. Under the steam-starved conditions of test HI-3, metallic Zircaloy — an efficient getter for antimony — existed throughout the test.

The cesium deposition profiles show peaks typical of the condensation of species that are volatile at the thermal gradient tube inlet temperature. Cesium was present in great excess over such electronegative fission products as Se, Br, Sb, Te, and I, so most of it must have existed as oxide or hydroxide species. Quantitatively, Cs_2O or CsOH are too volatile (11) to produce the peaks seen; the cesium-oxygen compounds may have contained other elements, such as carbon or tungsten (from the induction furnace susceptor), molybdenum (fission product), zirconium (cladding), or sulfur (ceramics). Apart from carbon, all these elements have been detected on the thermal gradient tube by spark source mass spectrometry (SSMS), in quantities sufficient to react with all the cesium.

The cesium deposits appeared to have two components; one component was soluble in basic leach and the other was insoluble. As illustrated in Fig. 6, the insoluble form constituted 4 to 40% of the deposited cesium above 350°C, but only 0.2 to 0.4% below 350°C. In general, 60 to 70% of the cesium (and iodine) that entered the thermal gradient tube passed through and was collected on the filters. This material was probably an aerosol that nucleated in the cooling gas as it flowed down the thermal gradient tube.

The iodine profile from each experiment exhibited only one peak, indicating one dominant release form. This release form appeared to be less volatile than pure CsI (12); the condensed phase may have been a solid solution of CsI in other cesium compounds, which reduced the vapor pressure of CsI. Because iodine has a lower fission yield than cesium, its presence did not affect the deposition behavior of cesium. As shown in Table 3, most of the released iodine deposited on the thermal gradient tubes and filters in all three tests. Less than 0.5% reached the heated charcoal where elemental or organic iodine forms would be collected.

The silver profile was measurable only in test HI-2. This profile may have resulted from the deposition of elemental silver (behaving like antimony) with a superimposed peak of a volatile silver compound. Alternatively, a silver aerosol may have deposited uniformly on the platinum; in this case the silver might have been fixed in place (resistant to nitric acid leaching of the individual sections) at the higher-temperature end but dissolved by the leach at the lower-temperature end.

Spark source mass spectrometry (SSMS) was used to obtain data for other elements because only a limited number of the elements that may be released from the furnace to the collection system can be measured by gamma spectrometry. However, due to the nature of the analyses, and also because of sample collecting limitations, this method (SSMS) provides data of lower accuracy (estimated to be about a factor of 3); but we obtain data for several important elements which are not otherwise available.

In test HI-3, SSMS smear samples on graphite electrodes were taken from five locations along the thermal gradient tube liner and from the glass wool prefilter. The results of these analyses, which are summarized in Fig. 7, are based on either the amount of ^{137}Cs, as measured by gamma spectrometry, or on a known quantity of erbium, which was added to solution samples as a standard. These data are typical of all three tests. As shown by the figure, total released material reached maximum concentrations near the higher temperature (inlet) end of the thermal gradient tube, whereas the fission products peaked near the center. Moreover, about 70% of the fission product mass passed through the thermal gradient tube to the filter, compared to about 35% of the less volatile nonfission products which were structural materials and impurities. Examination of the available data to estimate aerosol production, presented in Table 4, shows that of the mass of material released from the furnace, ~30% was collected on the thermal gradient tube and ~70% was collected on the filters in all three tests. The estimated aerosol concentrations show the expected increase with temperature.

Several transverse sections of each fuel specimen have been examined metallographically; the results are used to verify test conditions and to relate fuel damage to release behavior. The progressive oxidation of the Zircaloy cladding with increasing temperature is illustrated in Fig. 8, which compares an untested specimen with sections from tests HI-1 (1400°C) and HI-2 (1700°C). At the lower temperature about 40% of the cladding was converted to ZrO_2 by steam oxidation, but at 1700°C cladding oxidation was essentially complete. In both cases, however, the cladding was extremely brittle and suffered some fracturing during removal from the furnace. In test HI-3 the Zircaloy cladding was melted at about 1750°C (13); the melt caused dissolution of UO_2

and fusion to the ZrO_2 boat, which prevented the fuel specimen from being removed from the ZrO_2 furnace tube. The tube was filled with epoxy resin to stabilize the degraded specimen during handling. Subsequently, the assembly was sectioned transversely at 1-in. intervals for examination. The UO_2 fuel had retained its original circular shape only at the inlet end where the temperature was slightly lower. The remainder of the specimen consisted of broken and partially dissolved UO_2 on a puddle of formerly molten Zircaloy. A view of this degraded cladding/fuel mixture is shown in Fig. 9.

SUMMARY AND CONCLUSIONS

These three tests have provided additional data on fission product release under LWR accident conditions in a temperature range (1400-2000°C) where only limited data previously existed. In Fig. 10 our release rate data are compared with curves from a recent NRC-sponsored review (14) of available fission product release data. Only the curves for the more volatile elements are shown. Although the iodine release in test HI-3 was inexplicably low, the other data points for Kr, I, and Cs fall reasonably close to the corresponding curve, thereby tending to verify the NRC review. Further investigation of potential iodine deposition locations in that test is underway. The limited data for antimony and silver release fall below the curves in Fig. 10 by varying amounts; since we could not analyze for these elements at all apparatus locations, low values were not unexpected. The on-line release rate data for krypton and cesium are consistent with current understanding of the temperature dependent release mechanisms.

The results of spark source mass spectrometric analyses were in general agreement with the gamma spectrometric results and provided some additional data. Nonradioactive fission products such as rubidium and bromine appeared to behave like their chemical analogs cesium and iodine. The SSMS data indicated that much less tellurium and silver were released to the thermal gradient tube in test HI-3 (2000°C, partially oxidized Zircaloy) than in HI-2 (1700°C, completely oxidized Zircaloy); gamma spectrometry showed similar results for silver and antimony. These results, along with thermal gradient tube profiles and thermodynamic data, suggest that Te, Ag, Sn, and Sb are released from the fuel in elemental form. All are known to combine with metallic Zircaloy; apparently they are effectively retained up to ~2000°C, but are released at lower temperatures if the Zircaloy is completely oxidized.

Analysis of the cesium and iodine profiles in the thermal gradient tube indicates that iodine was deposited as CsI along with some other less volatile cesium compound. Cesium behavior is more complex. Because of the large amount of cesium released, oxide and/or hydroxide species must be present. The cesium profiles and chemical reactivity indicate the presence of more than one cesium species; cesium-oxygen compounds containing other fission products (Mo or Zr) or apparatus contaminants (S, C, or W) appear to be possible.

Studies of the microstructures of the fuel specimens showed changes consistent with test conditions: cladding fracturing, oxidation, and melting; fuel-cladding interaction to form U-Zr-O phases and cause UO_2 destruction; and gas bubble growth and coalescence to accelerate fission product release from the UO_2 (15).

REFERENCES

1. R. A. Lorenz, J. L. Collins, A. P. Malinauskas, M. F. Osborne, and R. L. Towns, Fission Product Release from Highly Irradiated LWR Fuel Heated to 1300-1600°C in Steam, NUREG/CR-1386 (ORNL/NUREG/TM-346) (November 1980).

2. R. A. Lorenz, J. L. Collins, M. F. Osborne, R. L. Towns, and A. P. Malinauskas, Fission Product Release from BWR Fuel Under LOCA Conditions, NUREG/CR-1773 (ORNL/NUREG/TM-388) (July 1981).

3. H. Albrecht and H. Wild, "Investigation of Fission Product Release by Annealing and Melting of LWR Fuel Pins in Air and Steam," Proceedings of Topical Meeting on Reactor Safety Aspects of Fuel Behavior, Sun Valley, Idaho, August 2-6, 1981.

4. H. Albrecht and H. Wild, "Behavior of I, Cs, Te, Ba, Ag, In, and Cd During Release from Overheated LWR Cores," Proceedings of the International Meeting on Light-Water Reactor Severe Accident Evaluation, Cambridge, Mass., Aug. 28-Sept. 1, 1983.

5. M. F. Osborne and G. W. Parker, The Effect of Irradiation on the Failure of Zircaloy-Clad Fuel Rods, ORNL-TM-3626 (January 1972).

6. M. F. Osborne, R. A. Lorenz, J. R. Travis, and C. S. Webster, Data Summary Report for Fission Product Release Test HI-1, NUREG/CR-2928 (ORNL/TM-8500) (December 1982).

7. M. F. Osborne, R. A. Lorenz, J. R. Travis, C. S. Webster, and K. S. Norwood, Data Summary Report for Fission Product Release Test HI-2, NUREG/CR-3171 (ORNL/TM-8667) (in reproduction).

8. M. F. Osborne, R. A. Lorenz, K. S. Norwood, J. R. Travis, and C. S. Webster, Data Summary Report for Fission Product Release Test HI-3, NUREG/CR-3335 (ORNL/TM-8793) (in preparation).

9. I. Barin and O. Knacke, Thermochemical Properties of Inorganic Substances, Springer-Verlag, p. 659, 1973.

10. M. Hansen, Constitution of Binary Alloys, pp. 2238-39, McGraw-Hill, 1958.

11. J. L. Collins, Oak Ridge National Laboratory, personal communication of calculation using JANAF data, January 1983.

12. I. Barin and O. Knacke, Thermochemical Properties of Inorganic Substances, Springer-Verlag, p. 254, 1973.

13. P. Hofmann, D. Kerwin-Peck, and P. Nikolopolous, "Physical and Chemical Phenomena Associated with the Dissolution of Solid UO_2 by Molten Zircaloy-4," Proceedings of the Sixth International Conference on Zirconium in the Nuclear Industry, June 28–July 1, 1982, Vancouver, British Columbia, Canada.

14. Technical Bases for Estimating Fission Product Behavior During LWR Accidents, NUREG-0772, U.S. Nuclear Regulatory Commission (June 1981).

15. R. V. Strain, Argonne National Laboratory, personal communication, April 1983.

Table 1. ANALYTICAL TECHNIQUES FOR FISSION PRODUCT RELEASE DATA

Technique	Time	Location	Elements detected
Gamma spectrometry	Pretest, posttest	Fuel specimen	Long-lived, high E, fission products — Cs, Sb, Ru, Eu, Ce
	On-line	Thermal gradient tube, filters, gas traps	Cs, Kr
	Posttest	Furnace components, thermal gradient tube, filters	Cs, Ag, Ru, Ce, Eu, (CO)
Activation analysis	Posttest	Charcoal, solution from furnace, thermal gradient tube, filters	I, Br
Spark source mass spectrometry	Posttest	Samples from furnace, thermal gradient tube, filters	All

Table 2. FUEL SPECIMEN AND TEST OPERATING DATA

	Test		
	HI-1	HI-2	HI-3
Fuel specimen data			
Length (cm)	20.3	20.3	20.3
Mass (g)	168.0[a]	166.0[a]	166.9[a]
Reactor	H. B. Robinson	H. B. Robinson	H. B. Robinson
Burnup (MWd/kg)	28.0	28.0	25.2
Krypton release during irradiation (%)	0.35	0.35	0.35
Test operating data			
Heatup rate (°C/min)	72	75	125
Maximum temperature (°C)	1400	1700	2000
Time at test temperature (min)	30.0	20.0	20.0
Average helium flow rate (L/min)[b]	0.436[c]	0.334	0.302
Average steam flow rate into furnace (L/min)	1.01	0.99	0.366
H_2 generated (L)[b]	12.17	13.54	4.92

[a] Including 30.7-g Zircaloy cladding and end caps.
[b] At STP.
[c] Argon was substituted for helium in tests HI-1 and HI-2.

Table 3. EXTENT AND DISTRIBUTION OF FISSION PRODUCT RELEASE FROM THREE TESTS OF H. B. ROBINSON FUEL

Test component or collector	Temperature or range (°C)	Fraction of fuel inventory found (%)				
		^{85}Kr	^{137}Cs	^{129}I	^{125}Sb	^{110m}Ag
Test HI-1 (30 min at 1400°C in steam at 1.0 L/min)						
Furnace	1400–900	0	0.79	0.016	0.0011	0
Thermal gradient tube[a]	800–130	0	0.58	0.83	~0.017[b]	0
Filters	~130	0	0.38	1.18	0[c]	0
Hot charcoal	~130	0	0	0.010	0	0
Cold charcoal	-78	2.83	0	0	0	0
Totals		2.83	1.75	2.04	0.018	0
Test HI-2 (20 min at 1700°C in steam at 1.0 L/min)						
Furnace[a]	1700–1000	0	8.82	~0.14	0.68	0
Thermal gradient tube	1000–150	0	15.5	16.8	~0.85[b]	1.86
Filters	~150	0	26.2	35.9	0.005	0.26
Hot charcoal	~150	0	10^{-6}	0.187	0	0
Cold charcoal	-78	51.5	0	0	0	0
Totals		51.5	50.5	53.0	1.53	2.12
Test HI-3 (20 min at 2000°C in steam at 0.36 L/min)						
Furnace[d]	2000–1000	0	13.5	0.60	10^{-3}	0.015
Thermal gradient tube	900–140	0	15.7	12.4	0	0
Filters	~140	0	28.5	22.4	0	0
Hot charcoal	~140	0	10^{-7}	10^{-3}	0	0
Cold charcoal	-196	59	0	0	0	0
Totals		59	57.7	35.4	10^{-3}	0.015

[a] In addition, particles of fuel and/or cladding recovered from the furnace contained significant amounts of ^{137}Cs, ^{125}Sb, ^{106}Ru, and ^{60}Co.

[b] Measured only after >90% of the Cs activity had been removed by leaching.

[c] Not detected because of high Cs activity, possibly as high as 0.08%.

[d] Fuel specimen could not be removed from ZrO_2 furnace tube and end plug. Because some released material remained with fuel and could not be measured, these values represent minima only.

Table 4. AEROSOL DATA FROM FISSION PRODUCT RELEASE TESTS

Test No.	Temperature (°C)	Cesium release (%)	Aerosol collected (mg)		Aerosol[a] concentration (g/m^3)	
			On thermal gradient tube	On filters	At furnace temperature	At 100°C
HI-1[b]	1400	1.75	~7	~18	~0.1	~0.4
HI-2[b]	1700	50.5	~90	~230	~1.6	~7
HI-3[c]	2000	57.7	80	220	2.5	15

[a] Assumes test time plus 5 min for aerosol production time.
[b] Mass of deposits estimated from SSMS data.
[c] Mass of deposits determined by weighing components.

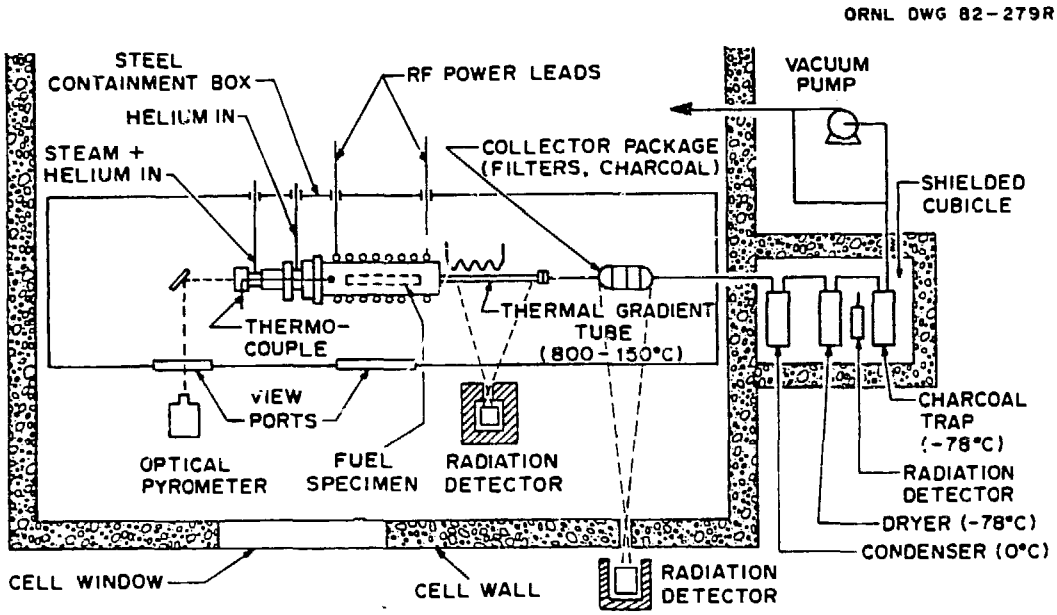

Fig. 1. FISSION PRODUCT RELEASE AND COLLECTION SYSTEM.

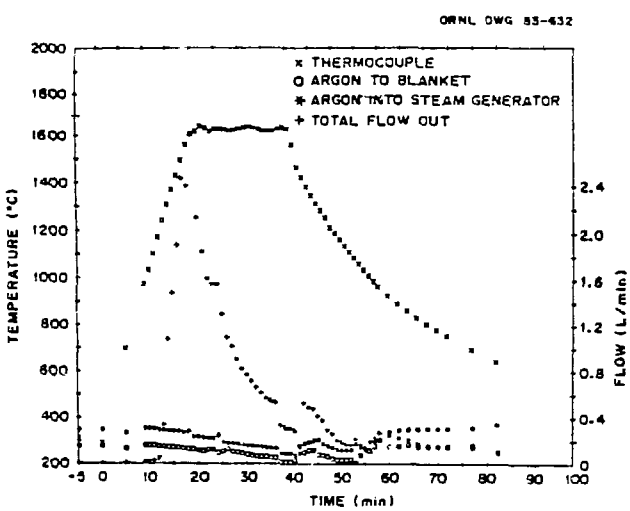

Fig. 2. TEMPERATURE AND FLOW HISTORY OF TEST HI-2.

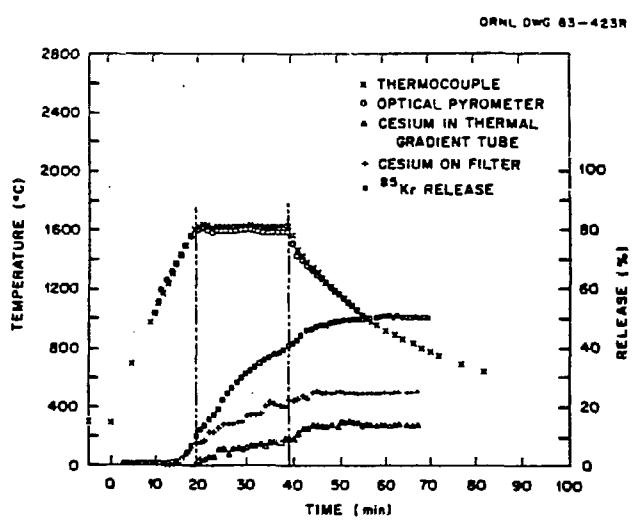

Fig. 3. RELEASE OF CESIUM AND KRYPTON AS FUNCTIONS OF TIME AND TEMPERATURE IN TEST HI-2.

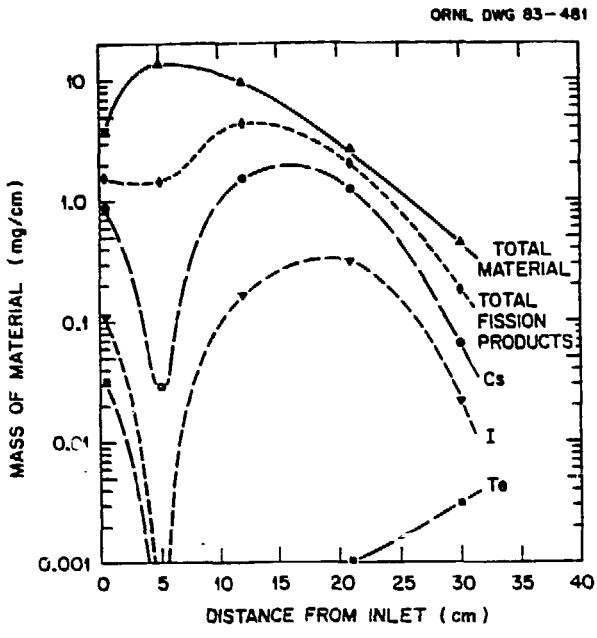

Fig. 4. DISTRIBUTION OF FISSION PRODUCTS IN TEST HI-2.

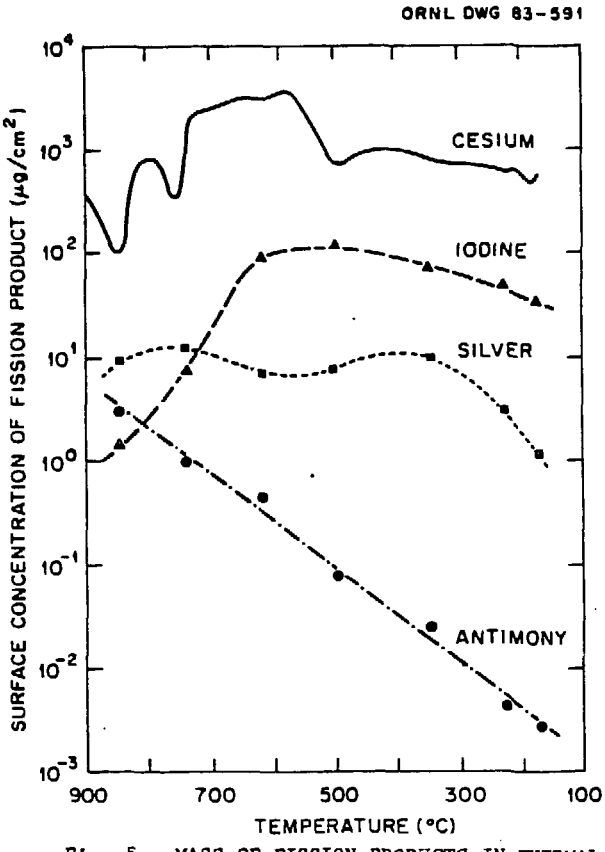

Fig. 5. MASS OF FISSION PRODUCTS IN THERMAL GRADIENT TUBE AFTER HI-2.

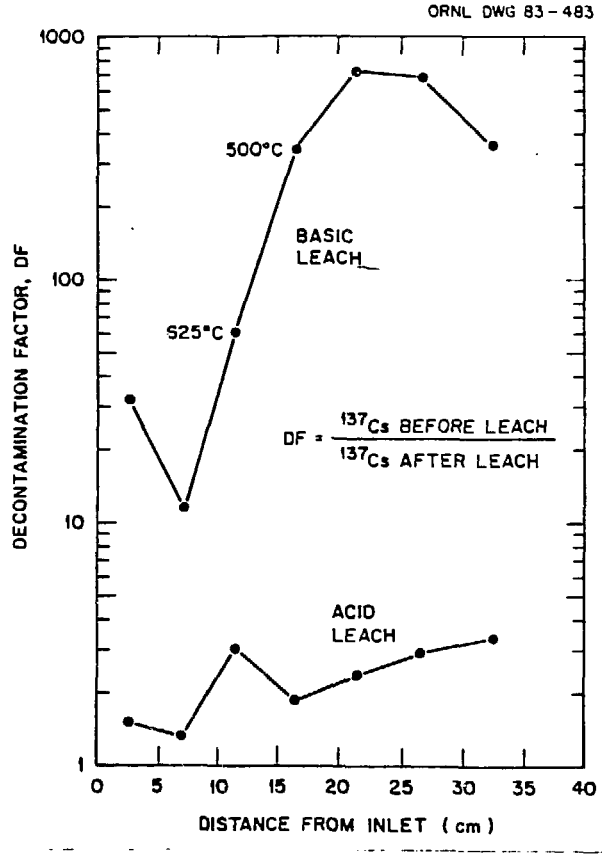

Fig. 6. SOLUBILITY OF CESIUM DEPOSITED IN THERMAL GRADIENT TUBE OF TEST HI-2: COMPARISON OF BASIC AND ACIDIC LEACHES.

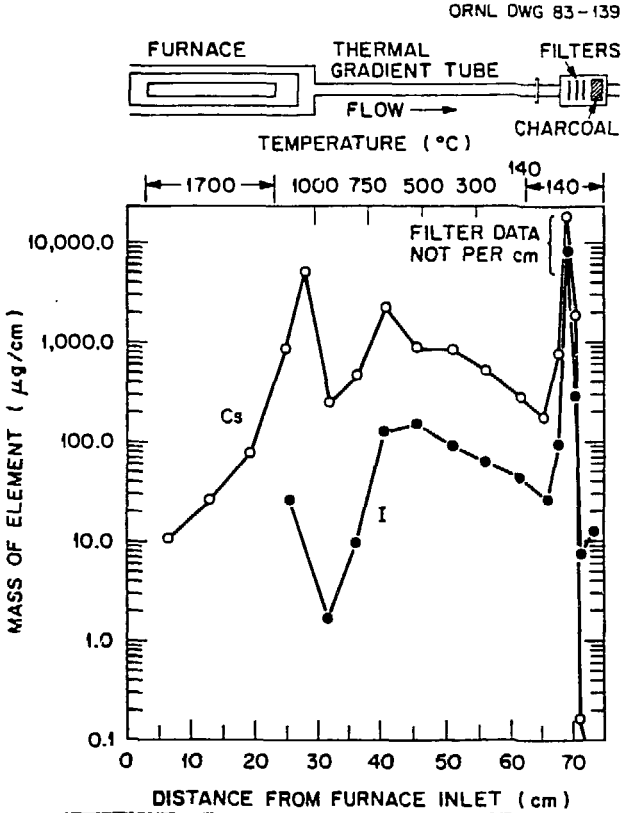

Fig. 7. DISTRIBUTION OF FISSION PRODUCTS AND TOTAL DEPOSITED MATERIAL IN TEST HI-3 THERMAL GRADIENT TUBE, AS INDICATED BY SSMS ANALYSES.

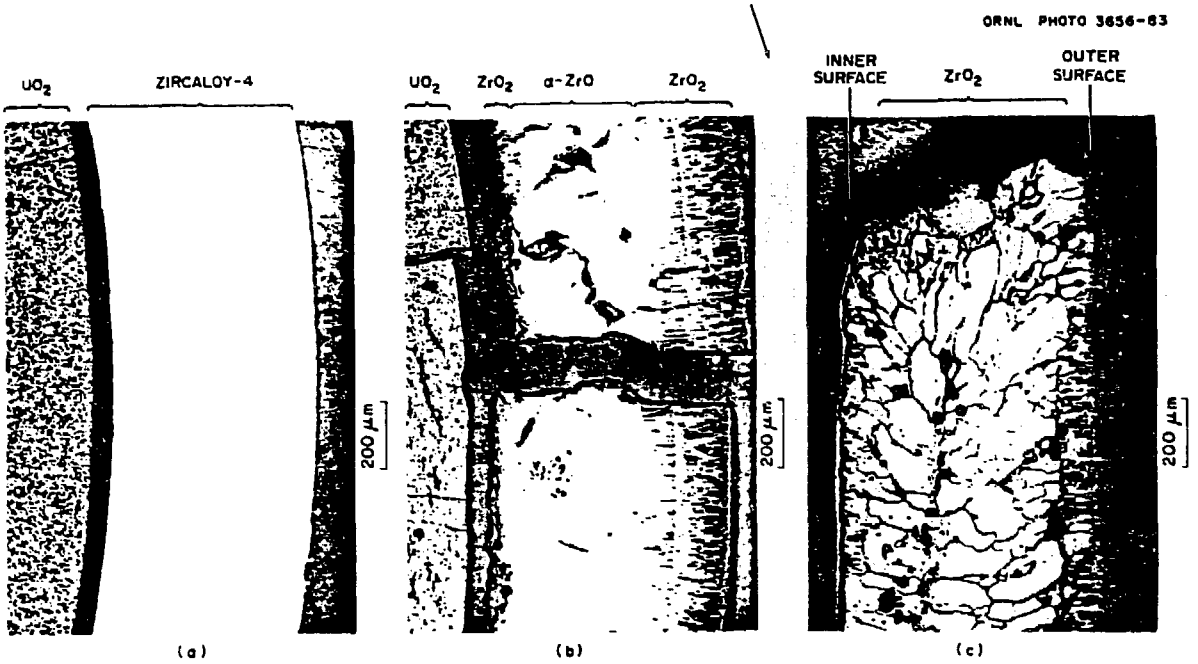

Fig. 8. COMPARISON OF CLADDING APPEARANCE IN IRRADIATED BUT UNTESTED CONTROL SPECIMEN (a) WITH PARTIALLY OXIDIZED CLADDING IN TEST HI-1 (b) AND FULLY OXIDIZED CLADDING IN TEST HI-2 (c). NOTE THE FRACTURES, THE INCREASE IN THICKNESS WITH OXIDATION, AND THE ZrO_2 AND α-ZrO LAYERS RESULTING FROM TESTING.

Fig. 9. VIEW OF MIDLENGTH REGION OF FUEL SPECIMEN FROM TEST HI-3, SHOWING EXTENSIVE MELTING AND INTERACTION OF ZIRCALOY CLADDING AND UO_2 FUEL. WITH THE EXCEPTION OF SMALL CHIPS, NO INTACT UO_2 WAS FOUND IN THIS REGION.

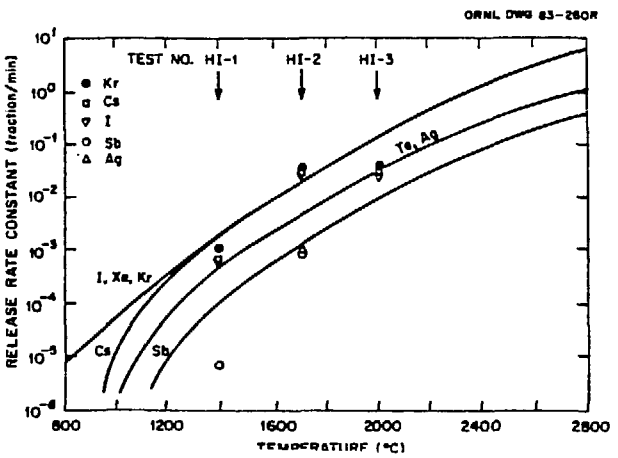

Fig. 10. RELEASE RATE DATA FROM TESTS HI-1, HI-2, AND HI-3, COMPARED TO CURVES FROM NUREG-0772.

DISCLAIMER